RAPID COMMUNICATIONS

Diamagnetic fields due to finite-dimension intense beams in high-gain free-electron lasers

J. B. Rosenzweig and P. Musumeci
Department of Physics and Astronomy, University of California at Los Angeles, 405 Hilgard Avenue, Los Angeles, California 90095-1547

(Received 19 May 1998)

High-gain, self-amplified spontaneous emission free-electron lasers (SASE FEL's), with proposed operation in wavelengths extending down to x rays, require intense relativistic electron beams, which under certain conditions can generate large diamagnetic fields. The action of these fields has the potential to seriously degrade FEL performance. It is shown here by both analysis and simulation that the finite size of the electron beams diminishes this effect so that it is negligible for proposed SASE FEL's. [S1063-651X(98)50709-X]

PACS number(s): 41.60.Cr, 41.60.Ap

The proposal to use high-gain, self-amplified spontaneous emission free-electron lasers (SASE FEL's) as coherent, high power radiation sources with wavelengths extending into the x-ray region [1,2] has been the subject of intense scrutiny recently. Initial laboratory results [3–5] have, within the range of experimental certainty, verified many of the basic theoretical and computational models for the SASE process. There are many diverse phenomena important in SASE FEL's, such as start-up from noise, fluctuations, and beam microbunching [6], to name a few. All of these effects have been investigated seriously, and included in theoretical models, but recently a new issue has been raised, that of the possible generation of a diamagnetic field by the transverse current associated with the beam's undulating motion. This possibility, recently brought to the fore by Freund and Antonsen [7], introduces potentially serious physics issues that are outside of the current model of the FEL interaction. The initial calculation of the diamagnetic fields for present and proposed SASE FEL's, which was performed for a beam that is infinitely wide and long, predicted field values that would have completely degraded the SASE FEL action. An extension to this calculation, in which the finite length of the beam is taken into account, was recently performed in a harmonic analysis by Freund and Tatchyn [8]. They found that the value of the diamagnetic field is diminished in the pulsed beam case by a factor of approximately L_b/λ_w with respect to the infinite beam, where $\lambda_w = 2\pi/k_w$ is the undulator wavelength and L_b is the bunch length. This analytically predicted effect has been verified here using numerical simulations, which are discussed below.

We begin our analysis of the diamagnetic field generation by examining the effects of the finite transverse extent of the beam on the field produced. The physical model used in the beam-wiggler (or undulator) magnet interaction is displayed in Fig. 1. The relativistic electron beam of energy $\gamma m_e c^2$ and uniform charge density ρ_0 out to a hard cutoff radius a passes through a planar wiggler of midplane field

$$B_{y,w} = B_0 \cos(k_w z). \tag{1}$$

In response to this field, the beam performs sinusoidal undulations in the x dimension, which for all cases of interest have amplitude much less than the beam size,

$$\varepsilon = \frac{e\beta B_0}{\gamma m_e c^2 k_w^2} \equiv \frac{a_w}{\gamma k_w} \ll a. \tag{2}$$

One additional strong inequality should be noted here, that the radial beam size is always much smaller than the wiggler wavelength, $k_w a \ll 1$. It should also be stated at this point that this analysis differs in two fundamental ways from that in Refs. [7] and [8] in addition to the inclusion of finite beam radius effects. The first is that the wiggler, like all present and proposed high-gain SASE FEL magnets, is planar in our case, and not helical, as in earlier analyses. The second is that we assume, and justify *ex post facto*, that the diamagnetic effects are very small, and thus we may ignore their possible effects on the beam motion.

The smallness of the beam centroid oscillations allows us to model the beam charge distribution as merely the uniform density beam, with a surface charge density that is sinusoidally varying in the main direction of propagation z,

$$\rho = \rho_0 + \rho_0 \varepsilon \cos(k_w z)\cos(\phi)\delta(r-a), \quad r \leq a. \tag{3}$$

The current density distribution associated with this charge distribution is

$$\vec{J} = \rho_0 \beta c \{[1+\varepsilon \cos(k_w z)\cos(\phi)\delta(r-a)]\hat{z} + k_w \varepsilon \sin(k_w z)\hat{x}\}, \quad r \leq a. \tag{4}$$

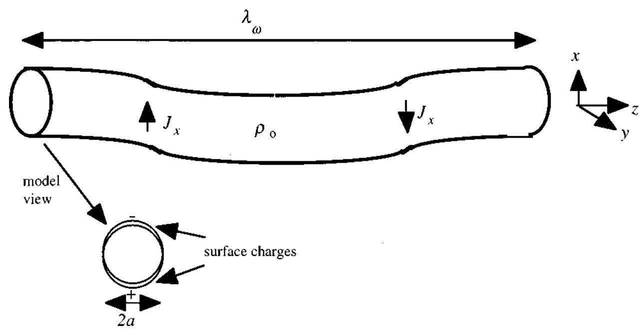

FIG. 1. Geometry for the model calculation, with a uniform density beam undulating at an amplitude smaller than the beam size, and polarization of the beam charge developing.

It is straightforward to show, by examining the relationship between the electrostatic potential and longitudinal component of the electromagnetic potential, under condition of time-independent flow, that all charges involved in creating *longitudinal* currents produce electric fields $E_{x,l}$ with an associated magnetic field $B_{y,l}$, such that the net horizontal force is

$$F_{x,l}=-e(E_{x,l}+\beta B_{y,l})=-\frac{eE_{x,l}}{\gamma^2}. \tag{5}$$

These are the so-called velocity fields that are familiar from the theory of charged particle radiation [9]. It should also be noted here that these fields are all derivable from the longitudinal component of the vector potential A_z. The ''space-charge'' force given in Eq. (5) has a strongly diminishing, well-known dependence on energy, and is for our case, in the limit $k_w a \ll 1$,

$$F_{x,l}=\frac{2\pi e\rho_0}{\gamma^2}[x+\varepsilon\ \cos(k_w z)]. \tag{6}$$

The first term in this expression is the usual defocusing space-charge force, while the second is a polarization term due to the transverse charge displacement. Because of the γ^{-2} dependence of this force, for the high energies employed in short-wavelength FEL's ($\gamma \geqslant 1000$) it is not of great importance.

In contrast, the *transverse* (horizontal) currents produce the so-called acceleration fields, which are qualitatively different from rectilinear space charge—the diamagnetic fields of present interest. To solve for these fields, we first write the equation for the horizontal component of the vector potential

$$[\vec{\nabla}_\perp^2-k_w^2]A_x=-\frac{4\pi}{c}\rho_0\beta c k_w\varepsilon\ \sin(k_w z). \tag{7}$$

This equation has a particular solution inside of the beam,

$$A_{x,p}=\frac{4\pi\rho_0\beta\varepsilon}{k_w}\sin(k_w z),\quad r\leqslant a, \tag{8}$$

and a vanishing potential outside of the beam. This is of course the infinite beam width solution, which gives the impressively large diamagnetic effect predicted by Freund and Antonsen [7]. Fortunately, inclusion of the homogeneous solution,

$$A_{x,h}=\begin{cases} CI_0(k_w r), & r\leqslant a,\\ DK_0(k_w r)+EI_0(k_w r), & r>a,\end{cases} \tag{9}$$

where C, D, and E are constants determined by application of the appropriate boundary conditions, lowers this value dramatically. To see this, we invoke continuity of the potential and field at $r=a$, and use vacuum boundary conditions at $r=\infty$, which gives (again taking $k_w a \ll 1$) the potential inside the beam,

$$\begin{aligned} A_x&=\frac{4\pi\rho_0\beta\varepsilon}{k_w}[1-k_w aK_1(k_w a)I_0(k_w r)]\sin(k_w z)\\ &\cong\frac{4\pi\rho_0\beta\varepsilon}{k_w}\left(1-\left\{1+\frac{(k_w a)^2}{4}\left[2\ \ln\left(\frac{k_w a}{2}\right)+0.154\,43\right]\cdots\right\}\right)\sin(k_w z)\\ &\cong\left|\ln\left(\frac{k_w a}{2}\right)\right|2\pi\rho_0\beta\varepsilon k_w a^2\sin(k_w z)\\ &\cong 8\pi\rho_0\beta\varepsilon k_w a^2\sin(k_w z). \end{aligned} \tag{10}$$

In the last expression in Eq. (10) we have suppressed the radial dependence of the potential, as well as the gentle dependence of the logarithmic factor (which is near 4 for typical design parameters), and given the approximate on-axis value of the potential. It can be seen that the magnitude of the potential is lowered by inclusion of finite radial dimension relative to the infinitely wide beam case by a factor proportional to $(k_w a)^2$, which is by assumption very small. Inclusion of a conducting (normal magnetic field excluding) boundary at a cylindrical beam pipe of inner radius b does not significantly affect the result of Eq. (10), as it introduces a correction factor of $1-\frac{1}{2}[\ln(k_w b/2)+0.577](k_w a)^2$, which is very close to unity.

The diamagnetic field associated with the potential given by Eq. (10) is thus approximately

$$\begin{aligned} B_{y,d}&\cong-8\pi\rho_0\beta\varepsilon(k_w a)^2\cos(k_w z)\\ &\cong-\frac{8\pi\rho_0 a_w k_w a^2}{\gamma}\cos(k_w z). \end{aligned} \tag{11}$$

It is most instructive to write this diamagnetic field normalized to the wiggler field,

$$\frac{B_{y,d}}{B_{y,w}}\cong-\frac{8\pi e\rho_0 a^2}{\gamma m_e c^2}\cong\frac{8I_b}{\gamma I_0}\cong-2(\gamma k_p a)^2,\quad k_p^2=\frac{4\pi e\rho_0}{\beta^2\gamma^3 m_e c^2}, \tag{12}$$

and $I_0 \cong 17$ kA is the Budker current. The ratio is thus, for high energy, always much smaller than unity. Physically, the

TABLE I. Diamagnetic suppression factors for various current and proposed SASE FEL's.

FEL	$B_{v,d}/B_{v,w}$
UCLA/LANL	6×10^{-4}
VISA	1×10^{-4}
TTF-FEL	1×10^{-5}
LCLS	3×10^{-7}

fields here have a natural radial spread of k_w^{-1}, as seen in Eq. (9), and thus are proportional to k_w^2, but in Eq. (12) k_w has, ignoring logarithmic dependence, canceled out of the expression for the normalized diamagnetic fields. This is ultimately because the beam displacement in Eq. (2), which gives rise to the diamagnetic current, is proportional to k_w^{-2}. In the approximations employed here, only the transverse beam dimensions normalized to $(\gamma k_p)^{-1}$ remain. The quantity k_p^{-1} is known commonly as the plasma skin depth, and is a measure of the length over which the beam, through its oscillatory plasma response, can naturally shield out external electromagnetic fields, and is also a measure of the strength of the plasma fields, $E,B\sim k_p^2$. In the case of a diamagnetic response, however, the fields do not scale as the more familiar plasma oscillation. The extra factor of γ multiplying the usual plasma wave number in Eq. (12) can be traced to the fact that the static diamagnetic fields, unlike space-charge fields, do not have an opposing electric field that cancels the net force as γ^{-2}, as in Eq. (5), and therefore the strength of the magnetostatic fields is proportional to $(\gamma k_p)^2$.

It is informative to attempt to include the suppression factor from longitudinal effects found in Ref. [8]. This analysis contains useful, physically interesting results, which are apparent after some inspection, such as a diminishing of the diamagnetic fields with frequency above $kL_b\approx1$, except for an expected enhancement of the fields near the FEL resonance, $k\approx2\gamma^2k_w$. Using these results, the maximum normalized diamagnetic field within the bunch, including longitudinal as well as radial effects, can be estimated as

$$\frac{B_{y,d}}{B_{y,w}}\cong\frac{k_wL_b}{\pi}(\gamma k_p a)^2. \tag{13}$$

Because of the dependence of the plasma frequency on the beam density, it can be seen that the relative diamagnetic field is, in the approximation given here, independent of beam dimensions, and depends only on the beam charge, energy, and wiggler wave number as $\sim Q_bk_w/\gamma$.

To illustrate the degree of diamagnetic suppression given in laboratory situations, we summarize in Table I the expected relative amplitude of the diamagnetic field of several present and proposed SASE FEL's: the UCLA/LANL experiment [5], which has achieved the highest single pass gain to date, the proposed visible SASE FEL experiment at BNL called VISA [10], the TTF-FEL [2], and the LCLS [1]. In all cases the diamagnetic fields have a negligible effect on all major aspects of the FEL operation. It should be noted, in contrast, that inclusion of only the longitudinal effects caused Freund and Tatchyn to conclude that the diamagnetic fields would have a large, measurable effect on the frequency spread of the LCLS radiation output.

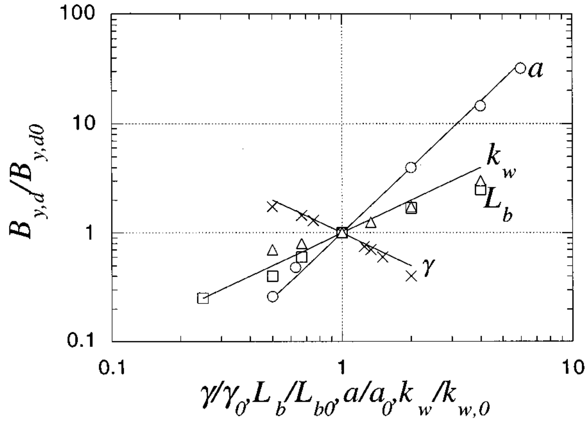

FIG. 2. On-axis diamagnetic fields obtained from TREDI simulation of a uniform density beam traversing an undulator, with approximate power-law predictions of Eq. (13) given by solid lines. Parametric simulations (L_b, U; a, O; k_w, Δ; γ, $\times$) were performed in the neighborhood of nominal UCLA/LANL experiment, $L_{b0}=3$ mm, $a_0=0.5$ mm, $k_{w0}=\pi$ cm^{-1}, and $\gamma_0=36$. The charge $Q=1.5$ nC for this case was scaled to keep a constant density for a and L_b variation.

To verify the predictions of the analysis developed here and in Ref. [8], we have performed numerical simulations of the diamagnetic fields using a multiparticle, three-dimensional Lienard-Wiechert field-solving computer code named TREDI [11]. In the simulations, a uniform density cylindrically symmetric beam of radius a and length L_b is launched into a wiggler field, with the diamagnetic fields evaluated on axis in the beam's longitudinal center after $3\lambda_w$ of propagation, in order to remove the effects of transient fields that dissipate with an observed characteristic length λ_w. The simulations are limited by numerical accuracy to moderate energies (<100 MeV); the energy and other relevant physical parameters varied over a range of values. The results of these parametric studies are summarized in Fig. 2, in which we plot the dependence of the calculated fields in the neighborhood of the nominal operating point of the UCLA/LANL experiment [5], for which we calculate $B_{y,d}/B_{y,w}\cong2\times10^{-4}$, in fairly good agreement with the analytical estimate of 6×10^{-4}. It is apparent from inspection of this log-log plot that the appropriate power laws are approximately obeyed, $B_{y,d}\propto a^2$, L_b, k_w, γ^{-1}, providing rough verification of the current analysis and that of Ref. [8]. A more detailed report of this numerical work, in which deviations from analytical results are studied, will be given in a forthcoming paper.

In conclusion, we have shown, by extending the results of Ref. [8] to include examination of radial effects, when all finite beams are taken into account, that the diamagnetic fields generated by the intense relativistic electron beam used in all relevant SASE FEL's are negligibly small. The conclusions of this analysis have been verified by use of numerical solutions of a finite beam distribution-derived fields, which include all time-dependent phenomena, such as finite pulse length and transient effects due to finite undulator length. A more systematic analysis of these effects will be undertaken in the future, with particular attention paid to understanding the radiated fields that are explicitly forbidden in the analytical model given here, but are present in the numerical simulations [12].

The problem analyzed here is also related to another as yet poorly understood effect in high-intensity electron-beam physics, that of the forces encountered by the beam electrons during bending, especially the wigglerlike bends encountered in chicane compressors [12]. We also intend to apply methods used in this analysis, in particular the numerical simulations, to give insight into this problem, which has the potential to seriously degrade the performance of devices using compressors, such as FEL's and linear colliders.

The authors acknowledge useful discussions with H.Freund, L. Giannessi, M. Hogan, and C. Pellegrini. The work was supported by the U. S. Department of Energy under Grant No. DE-FG03-93ER0796, and the Alfred P. Sloan Foundation under Grant No. BR-3225.

[1] R. Tatchyn *et al.*, Nucl. Instrum. Methods Phys. Res. A **375**, 274 (1996); C. Pellegrini *et al.*, *ibid.* **331**, 223 (1993).

[2] B. Faatz *et al.*, Nucl. Instrum. Methods Phys. Res. A **375**, 441 (1996).

[3] J. Gardelle, J. Labrouch, and J. L. Rullier, Phys. Rev. Lett. **76**, 4532 (1996).

[4] Initial SASE experiments at BNL reported by I. Ben-Zvi (private communication).

[5] M. Hogan *et al.*, Phys. Rev. Lett. **80**, 289 (1998); ultrahigh gain UCLA/LANL experiment reported in M. Hogan *et al.* (unpublished).

[6] J. B. Rosenzweig, G. Travish, and A. Tremaine, Nucl. Instrum. Methods Phys. Res. A **365**, 255 (1995); the experimental measurement of coherent transition radiation predicted here is reported in A. Tremaine *et al.* (unpublished).

[7] H. P. Freund and T. M. Antonsen, Jr., *Principles of Free-electron Lasers*, 2nd ed. (Chapman & Hall, London, 1996).

[8] H. P. Freund and R. Tatchyn (unpublished).

[9] J. D. Jackson, *Classical Electrodynamics* (Wiley, New York, 1975).

[10] C. Pellegrini (private communication).

[11] F. Ciocci, L. Giannessi, A. Marranca, L. Mezi, and M. Quattromini, Nucl. Instrum. Methods Phys. Res. A **393**, 434 (1997).

[12] B. E. Carlsten and T. O. Raubenheimer, Phys. Rev. E **51**, 1453 (1995).